

# Compensation Tracker: Data Association Method for Lost Object

Zhibo Zou\*      Junjie Huang\*      Ping Luo<sup>†</sup>

School of Automation, Chongqing University of Posts and Telecommunications, Chongqing,  
400065, China

{s190331072, s190331071}@stu.cqupt.edu.cn,  
{luoping}@cqupt.edu.cn

**Abstract:** At present, the main research direction of multi-object tracking framework is detection-based tracking method. Although the detection-based tracking model can achieve good results, it is very dependent on the performance of the detector. The tracking results will be affected to a certain extent when the detector has the behaviors of omission and error detection. Therefore, in order to solve the problem of missing detection, this paper designs a compensation tracker based on Kalman filter and forecast correction. Experiments show that after using the compensation tracker designed in this paper, evaluation indicators have improved in varying degrees on MOT Challenge data sets. In particular, the multi-object tracking accuracy reached 66% in the 2020 datasets of dense scenarios. This shows that the proposed method can effectively improve the tracking performance of the model.

**Keywords:** Multi-Object Tracking, Tracking Compensation, Kalman Filtering; Detector Omission

## 1. Introduction

Currently, multi-object tracking has been used in many scenarios. For example, intelligent security, automatic driving, pedestrian tracking, intelligent monitoring and so on. In the network framework, detection-based tracking is the mainstream multi-object tracking model.

Detection-based tracking can be traced back to DeepSort[4], which used the detection results of YOLOv3[18] as a tracking benchmark, and introduced a Re-ID model specifically for extracting appearance information as a further matching optimization. Moreover, it uses cascading matching and Hungarian algorithm [20] to match and process multiple unmatched object. This provides a tracking framework for future development. Subsequently, MOTDT[21] carries out tracking optimization processing on this basis. It uses the network to generate a score maps and score the trajectory of each tracked object. With the development of the detection field, the tracking field has been greatly influenced. JDE[5] tracker, while following the previous tracking method, combines the Re-ID model with the detection network to form a one-stage tracker. Moreover, it uses the new loss function for appearance learning and utilizes the automatic balance loss function to solve the multi-task learning problem of multi-object tracking. Due to the update and development of detectors, the increase of detection accuracy has great influence on tracking. In [22,3,23,24], they all apply new detectors or detection optimization methods to improve tracking performance. Of course, there are also other authors who innovate at other levels. IoU-tracker [16] only uses the boundary boxes intersection over union (IoU) of adjacent frames to track object. Although it achieves good results in speed, it is not accurate enough.

---

\*The first two authors contributed equally to this work.

<sup>†</sup>Corresponding author.

Detection-based tracking models can be divided into end-to-end and non-end-to-end. These end-to-end methods such as [31,34,35,36] use pipeline end-to-end tracking architecture, chain tracking architecture, and graph convolutional network architecture. This type of models usually completes the detection and tracking tasks in the network without introducing other object matching methods and trackers at the back end of the network. Those of non-end-to-end tracker such as [5,3] usually take the detection result of the network as the input of the back-end tracker and then use a series of prediction and matching methods to allocate, initialize tracking and move the object. Our approach is designed on the back-end tracker of the non-end-to-end models.

In addition, there are many methods of object tracking. [37,38,39] and others use networks or modules with memory functions such as RNN and LSTM to obtain long-term and short-term information of tracking object to prevent object loss and identity switching. [40,41,42], etc, integrate and utilize object features such as motion model, spatiotemporal model, and appearance model for extraction, prediction and correlation, thereby improving object tracking performance and alleviating the interference of similar object to tracking. These tracking methods are long-term tracking of the object without considering the issue of whether the lost object should also be tracked. In the detection-based tracking model, these methods will slow down the running speed. In a non-end-to-end model, these methods are not necessarily applicable.

For the detection-based tracking model, the detector plays a decisive role in the comprehensive performance of multi-object tracking. However, if the detector does not detect the object on a certain frame, but the object is actually present, it will directly lose the object. We believe that the tracker can not only use the information provided by the detector to match, but also use the past information to predict and compensate the missing object. Therefore, we design the compensation tracker and its forecast correction module to solve this problem. The effect of our compensation tracker is shown in Figure 1.

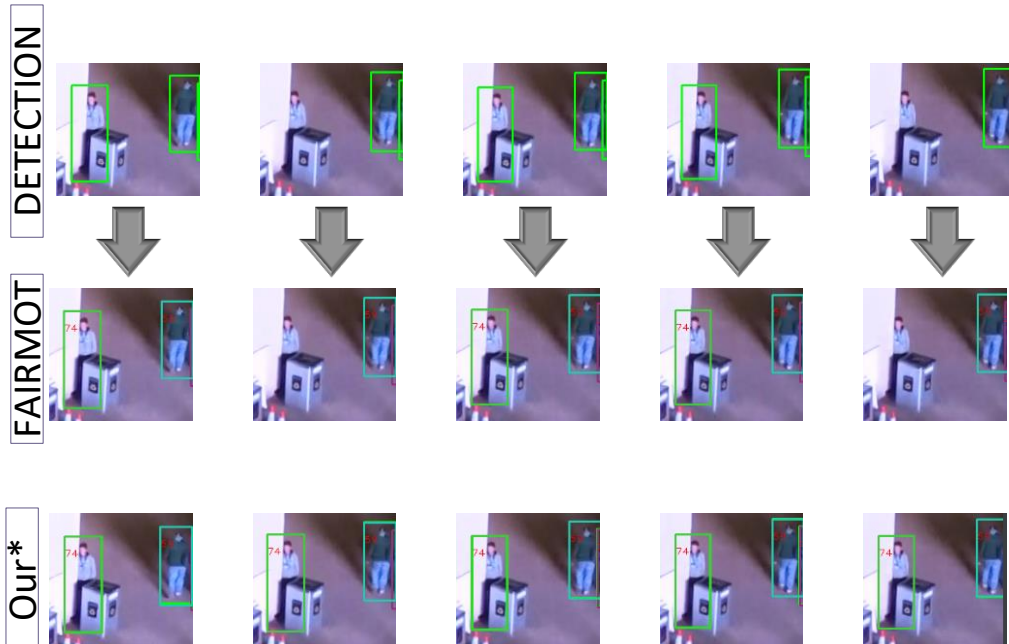


Figure 1. From top to bottom, these three lines are the detection results, the model tracking results and the results after using our compensation tracker, respectively. As can be seen in the figure, the

tracking model based on detection will have the problem of missed detection and unable tracking. And our tracker can make up for the problem of being unable to track due to missing detection by the detector.

## 2. Relate Works

**Detection Method based on Anchor-Free.** Anchor-based detection method[1,6,7,17] samples fixed shape bounding boxes around low-resolution images and classified each bounding box as 'foreground 'or' background '. At the same time, NMS and other methods are used to filter the bounding box, which will increase computation. In this paper, Anchor-Free detection method is adopted, which does not need the above complex operation. It uses heatmaps to extract local peaks [10, 11] and predicts the object center point, so as to predicts the object boundary based on the center point. This key points prediction method can greatly reduce the computation and object's ID switch [2].

**One-Stage Detection Model.** Previous tracking models usually treat object detection and Re-ID as two separate tasks. In [12,13,14,15], all interested object in the graph are firstly determined by the detector of convolutional neural network, and then the image is cut out according to the boundary box and fed into the identity embedding network to extract the re-id features. Then, the bounding box is then linked into multiple tracks [3,18]. These operations can increase the network computation and complexity and are not conducive to real-time tracking. In this paper, object detection and embedding functions are completed simultaneously in a single network and the model is non-end-to-end , as shown in Figure 2.

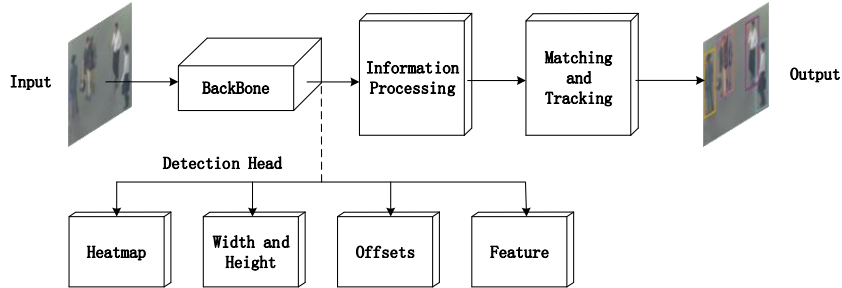


Figure 2. One-Stage detection and tracking network architecture

**Compensation Tracker.** At the present, the tracker is generally a sequential task, which calculates the cost matrix according to Re-ID and boundary box information and then uses Kalman filter [19] and Hungarian algorithm [20] to complete the prediction and assignment tasks. After the completion of the matching process, we will comprehensively process the object that are not tracked and matched in the current frame. We use the regression box, confidence and predicted boundary box (BBox) of these object to obtain a more accurate BBox and then compensate for the missing pedestrian tracking boundary box. Finally, the compensation result is output together with the previous matching result, as shown in Figure 4.

## 3. Methods

### 3.1 Baseline Network Model

We use FairMOT [3] as the baseline model to experiment. In this paper, we only use deep aggregation network (DLA)[9] as the backbone network. Moreover, the deformable convolution [12] (DCNv2) is applied to DLA network to expand the receptive field of the network and improve the

detection accuracy. Compared with the original DLA network, the DLA network with deformable convolution has more jumper layers, which can increase the receptive field and enhance the modeling ability [12], as shown in Fig. 3.

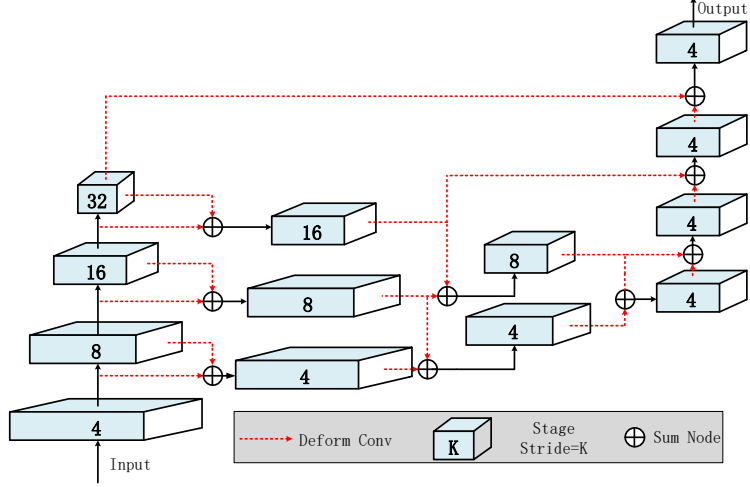


Figure 3. Backbone network structure(DLA-DCNv2-34)

### 3.2 Design of Compensation Tracker

This section will introduce how the compensation tracker predicts and solves the problem of the lost object caused by detector omission. The process flow of the tracker is shown in Figure 4. It consists of two parts: the Kalman filter Compensation (KC) and the Forecast Correction (FC)

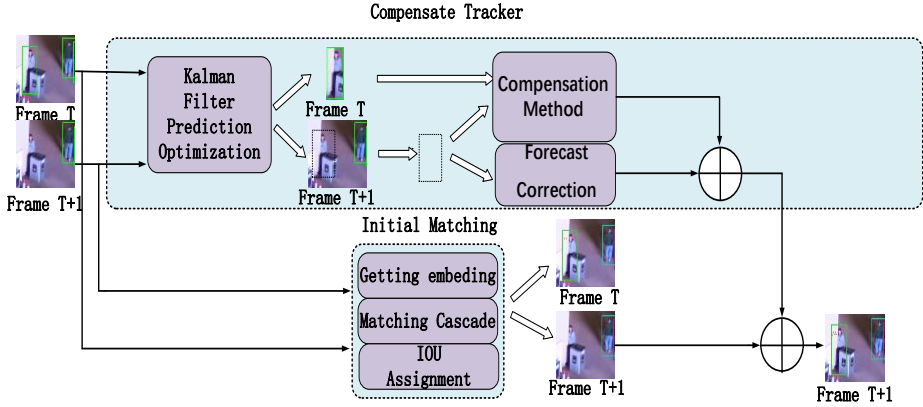


Figure 4. Compensation tracker (CT) processing. The figure above is for the case of lost object. When the object is tracked at frame T but is not detected at frame T+1, the object is sent to the compensation tracker for prediction and correction. Meanwhile, other object will still match and go on data association. Then, after comprehensively processing the prediction results, correction results and association results, the tracker outputs the final compensation results.

**Prediction and update method of Kalman filter.** In the prediction and update of the tracker, we use the Kalman filter with uniform motion and linear observation by default. Its' input can be defined as:

$$\mathcal{X} = [\alpha, \beta, \gamma, \delta, \dot{\alpha}, \dot{\beta}, \dot{\gamma}, \dot{\delta}] \quad (1)$$

Where  $\alpha$  and  $\beta$  are the horizontal and vertical coordinates of the BBox, respectively;  $\gamma$  is

the ratio of the width and height of BBox;  $\delta$  is the height of the BBox;  $\dot{\alpha}, \dot{\beta}, \dot{\gamma}, \dot{\delta}$  are the velocities of the corresponding components.  $[\alpha, \beta, \gamma, \delta]$  are directly observed as object states. Since the uncertainty of velocity relative to position and shape is higher, the initial state of each covariance for Kalman filter is as follows:

$$\begin{cases} \text{Conva} = \text{diag}([2\sigma_p\delta \ 2\sigma_p\delta \ 1e-2 \ 2\sigma_p\delta \ 10\sigma_v\delta \ 10\sigma_v\delta \ 1e-5 \ 10\sigma_v\delta]^T)^2 \\ Q = \text{diag}([\sigma_p\delta \ \sigma_p\delta \ 1e-2 \ \sigma_p\delta \ \sigma_v\delta \ \sigma_v\delta \ 1e-5 \ \sigma_v\delta]^T)^2 \\ R = \text{diag}([\sigma_p\delta \ \sigma_p\delta \ 1e-1 \ \sigma_p\delta]^T)^2 \end{cases} \quad (2)$$

Where  $\sigma_p$  is the standard deviation of position and  $\sigma_v$  is the standard deviation of velocity. R is the covariance matrix of the error between the estimated value and the true value; Q is the multi-variate normal distribution of covariance matrix.

Take the above information as input information and calculate the error covariance matrix between the calculated value and the real value at k-1 frame:

$$\widehat{\text{Mean}}_k = F_k \widehat{\text{Mean}}_{k-1} + A_k \mathcal{X}_k \quad (3)$$

$$\text{Cova}_k = F_k \text{Cova}_{k-1} F_k^T + Q \quad (4)$$

Where k represents the current frame number, k-1 is the previous frame number;  $F_k$  is the motion transformation matrix;  $A_k$  is the control parameter matrix;  $\mathcal{X}_k$  is the control quantity;  $\widehat{\text{Mean}}_k$  is the estimated value of the system state at frame K;  $\text{Cova}_k$  is the covariance matrix of the output. Then calculate the Kalman gain:

$$K_k = \text{Conva}'_k \cdot A_k^T \cdot (A_k \cdot \text{Conva}'_k \cdot A_k^T + R)^{-1} \quad (5)$$

$$\widehat{\text{Mean}}'_k = \widehat{\text{Mean}}'_k + K_k (Z_k - A_k \cdot \widehat{\text{Mean}}'_k) \quad (6)$$

Where  $K_k$  is the Kalman gain and  $Z_k$  is the system measurement value at k frame.  $\widehat{\text{Mean}}'_k$  is the calculated value from k-1 frame to K frame.  $\text{Conva}'_k$  is the covariance matrix of the error between the calculated value and the real value at k frame. [4,19]

Finally, the error covariance matrix between the estimated value and the real value is updated:

$$\text{Conva}_k = (1 - K_k \cdot A_k) \text{Conva}'_k \quad (7)$$

**Compensation Method.** After appearance matching and IoU matching, we store the missing object. And we predict the boundary box of the missing object through the above method, as shown in the dashed box in Figure 4. If the object is still in the tracked range, the missing object's bounding box is updated. Moreover, we have added the compensating confidence of the object, which is based on the initial confidence of the object. However, when the object has lost for many times, the compensation confidence will decrease, and if it has detected for many times, the compensation confidence will increase. We determine whether the lost object need to be compensated for tracking bounding box by setting the threshold of the compensation confidence

### 3.3 Forecast Correction Method of Compensation Tracker

In the experiment, we find that there are some defects in using only the prediction and update of Kalman filter to compensate unconditionally. In this section, we further introduce how to optimize the bounding box, including error bounding box (EBBox) suppression, boundary box offset correction, removing occluded and overlapped boxe and boundary elimination.

**Error Bounding Box Suppression.** EBBox is caused by the fact that the tracked object has been lost or the object has not been detected in many frames, but the boundary box compensation is still carried out. Therefore, we set the frame number of loss compensation within 30 and suppress the generation of EBBox by setting the threshold value of compensation

confidence for judgment. The experimental results show that the number of compensated frames can be set to 30 in a fixed scene and set [5,15] in a moving scene. We define compensation confidence as:

$$C = C_i - \eta * L_t + \theta * M_t \quad (8)$$

Where,  $C$  is the compensating confidence degree;  $C_i$  is the original confidence of the object boundary box;  $L_t$  is the number of missed object;  $M_t$  is the number of successful initial matches;  $\eta$  is the weight of the lost object number, which is set to 0.1 in the algorithm;  $\theta$  is the weight of the initial number of successful matches, which is set as 0.2 in the algorithm. As shown in B in Figure 5, when the compensation confidence is lower than the set threshold (0.5), the pedestrian bounding box of the object is filtered out.

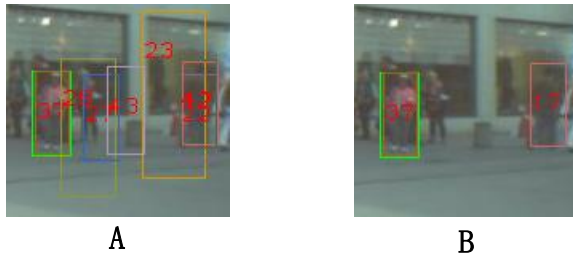


Figure 5. A represents that formula (8) is not added, and B represents that formula (8) is added. The green box represents the successful detection of the detector. It is obvious from the figure that after the compensation confidence is added, the bounding box that does not meet the condition will be filtered out, and the bounding box 17 is retained because it satisfies the formula condition.

**Boundary Elimination.** Experiments show that when the tracked scene moves relatively fast, only using the error bounding box suppression will not achieve the optimal effect. Therefore, when the object has disappeared in the image but the pedestrian bounding box still exists in the image, we need to judge the position of the center point of the pedestrian bounding box as follows:

$$\begin{cases} x - x_w * \alpha > 0 \\ \text{width} - x - x_w * \alpha > 0 \end{cases} \quad (9)$$

Where  $x$  is the center point of the bounding box;  $x_w$  is the width of the bounding box;  $\alpha$  is the weight of the bounding box width, which is set to 0.22 in the algorithm;  $\text{width}$  is the width of the image. When bounding box do not satisfy formula (9), the object pedestrian bounding box will be filtered out.

**Boundary Box Offset Correction.** Due to the inaccuracy of the border size in the predicted bounding box, the object cannot be marked accurately. In order to solve this problem, based on the position information of the boundary box calculated by Kalman filter, we use the input position information to calculate the error value between the predicted position information and itself. If the error is too large, the information of the bounding box needs to be weighted with the minimum error. Otherwise, the predicted bounding box can be used directly. What more, about predicting the size of the bounding box, we believe that the border size of adjacent frames changes very little. Therefore, in this part, the prediction box is calculated and compared with the bounding box tracked by the previous frame. We limit the area change of the prediction box within 1.015 times to prevent the border offset.

**Removing Occluded and Overlapped Box.** In order to improve the tracking accuracy, we also

eliminate the bounding box for pedestrian occlusion and pedestrian overlap to reduce the false detection rate. The effect can be seen in Figure 7 F. Our method uses the predicted initial



Figure 6. Schematic diagram of boundary suppression calculation. C is the effect picture before adding formula (9). D is the effect picture after adding formula (9). The width and height of the image are 640 and 480; the center point of the bounding box 12 is (43, 250) and the width is 195.73, and the center point of the bounding box 129 is (596, 242) and the width is 206.9. Since the bounding box 12 satisfy formula (9), the bounding box is retained. Since the bounding box 129 dose not satisfy the formula (9), it is filtered out.

bounding box  $\Phi$  and the tracked pedestrian bounding box set  $\mathcal{T}_T^i$  for comparison and judgment, including their area ratio, IoU, and bounding box embedding degree. The calculation formula of IoU is:

$$\text{IoU} = \frac{\Phi \cap \mathcal{T}_T^i}{\Phi \cup \mathcal{T}_T^i} \quad (10)$$

Here we use each predicted bounding box and all tracked pedestrian bounding boxes for IoU calculation.

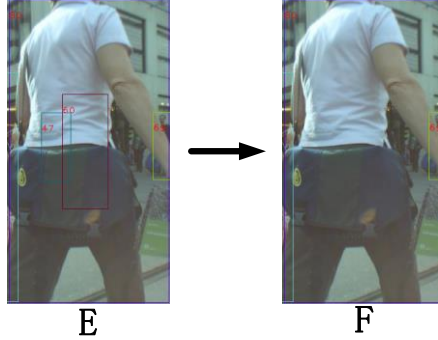


Figure 7. The comparison chart before and after using the overlapped and occluded suppression module. E is the effect diagram without using overlapped and occluded suppression module. F is the effect diagram after using this module. It is obvious from the figure that the wrong bounding boxes has been well suppressed.

## 4. Experiments

### 4.1 Experiments Detail

In the experiment, we use the datasets on MOT Challenge for testing. The platform provides

a variety of datasets. These datasets contain videos of different scenes including moving and fixed visual scenes. At the same time, the datasets include all kinds of scenes such as pedestrian

---

**Algorithm 1: Compensation Tracker**

---

**Input:** Lost object  $\mathcal{L} = \{l_i | l_i \in \{\mathcal{T}_T^i - \mathcal{D}_{T-1} \cap \mathcal{D}_T\}\}$  where  $\mathcal{D}_{T-1}, \mathcal{D}_T$  is object detection in

frame T-1 and T;

initialize Track  $\mathcal{T}_T$ .

$\sigma_a$ : Threshold of area change

$\sigma_i$ : IoU threshold

$\sigma_r$ : Area ratio

$\sigma_c$ : Threshold of compensation confidence

**Output:** Tracks  $\mathcal{T}_T$  of the video.

```

1  for  $l_k \in \mathcal{L}$  do:
2       $\mathcal{C} \leftarrow \text{Get\_Compensation\_Confidence}(l_k)$  by (8)
3      If  $\mathcal{C} > \sigma_c$ :
4           $\text{Mean}_k', \text{Conva}_k' \leftarrow \text{Get\_Estimated\_Value}(\text{Mean}_k, l_k, \text{Conva}_k)$  by (3),(4)
5           $K_k \leftarrow \text{Get\_Kalman\_gain}(\text{Conva}_k')$  by (5)
6           $\text{Mean}_k, \text{Conva}_k \leftarrow \text{Update\_Value}(K_k, \text{Mean}_k', \text{Conva}_k')$  by (6),(7)
7          If (8)  $\leftarrow \text{Mean}_k$ :
8              If  $\text{Calculate\_Areas}(\text{Mean}_k, l_k) > \sigma_a$ :
9                   $\text{Mean}_k \leftarrow \text{Areas\_scaling}(\text{Mean}_k, l_k, \text{Mean}, \sigma_a)$ 
10             end if
11         end If
12         for  $\mathcal{T}_T^l \in \mathcal{T}_T$  do:
13              $\text{IoU} \leftarrow \text{Calculate\_IoU}(\text{Mean}_k, \mathcal{T}_T^l)$ 
14              $\text{Areas} \leftarrow \text{Calculate\_Areas}(\text{Mean}_k, \mathcal{T}_T^l)$ 
15             If  $\text{IoU} > \sigma_i$  and  $\text{Areas} > \sigma_r$ :
16                  $\mathcal{C} = 0$ 
17             end If
18         end for
19          $l_k \leftarrow \text{Update\_Parameter}(\text{Mean}_k, \text{Conva}_k, \mathcal{C})$ 
20     end for
21     end If
22     If  $\mathcal{C} > \sigma_c$ :
23          $\mathcal{T}_T^{l+1}.append(l_k)$ 
24     end If

```

---

occlusion, pedestrian overlap, sparse pedestrians and dense pedestrians. We have conducted tests and evaluations on MOT2016[26], MOT2017[26] and the latest MOT2020[27]. And we achieved relatively good results and indicator data in these data sets.

**Experiment Platform.** Our experiment is implemented on Pytorch. The computer used in the experiment is Intel(R) i5-9400H CPU @2.9GHz and GTX1080Ti graphics card. Besides, we used the training model parameters of the DLA network for experiment. Regarding the frame number

compensation of CT, the value range of the frame number is [3,30] and the value of 30 is the best under fixed visual scenes. In a moving scene, the value depends on the moving speed of the tracking scenarios, but the value cannot be too small or it will affect the tracking effect. Among the related parameters, the upper limit of the compensation confidence depends on the compensation frame value. At the same time, the max number of reserved frames for lost targets cannot exceed 50. In particular, in the part of the occlusion and overlap suppression algorithm, the area ratio for judging whether they completely overlap is 0.9 and the IoU threshold is 0.95. When the bounding box is occluded and embedded, the IoU threshold is set to 0.05 and the area ratio is 0.5. Furthermore, the area change threshold of adjacent frames of the bounding box is set to 1.015. More importantly, because our tracker retains the original confidence of the lost object and increases the confidence of the compensation, the overall confidence range is now between 0.3 and 0.6 for the best results

**Evaluation Indicators.** Our experiment uses data indicators CLEAR Metrics [35] and IDF1, including multi-object tracking accuracy (MOTA), ID switching (ID Switch), the number of correct detections and the ratio of Ground True (IDF1), multi-object tracking accuracy ( MOTP), the most tracked object (MT), the most lost object (ML), the average number of false alarms per frame (FAF) and the number of times the tracking process is interrupted (Frag) [25].

## 4.2 Ablation Experiments

In this part, we will use the Compensation Tracker (CT) on different models. And the

Table 1: Module ablation experiment on MOT2020 Test. The best result for each indicator will be bold and red.

MOT2020 Test					
Component	MOTA↑	IDF1↑	MT↑	ML↓	ID.Sw↓
Baseline	58.7	63.7	<b>66.3%</b>	<b>8.5%</b>	6013
Baseline+KC	65.0	66.6	59.1%	13.0%	<b>2119</b>
Baseline+KC+FC	<b>66.0</b>	<b>67.0</b>	56.3%	13.3%	2237

Table 2: 'Private' model ablation experiment. '\*' means that the model data is evaluated by motchallenge-devkit. The best result for each indicator will be bold and red.

MOT2016 Test					
Models	MOTA ↑	IDF1 ↑	MT ↑	ML ↓	ID.Sw ↓
JDE[5]	64.4	55.8	20%	34%	1544
JDE with CT	<b>65.0</b>	<b>59.1</b>	<b>36.1%</b>	<b>18.8%</b>	<b>1525</b>
FairMOT[3]	68.7	70.4	39.5%	19.0%	953
FairMOT with CT	<b>69.8</b>	<b>71.1</b>	<b>42.0%</b>	<b>15.8%</b>	<b>912</b>

MOT2020 Train					
Models	MOTA ↑	IDF1 ↑	MT ↑	ML ↓	ID.Sw ↓
JDE[5]*	48.2	32.1	318	497	18631
JDE with CT	<b>54.4</b>	<b>43.1</b>	<b>526</b>	<b>372</b>	<b>11157</b>
FairMOT[3]*	62.3	47.5	790	288	16395
FairMOT with CT	<b>65.6</b>	<b>57.5</b>	<b>1030</b>	<b>247</b>	<b>7816</b>

network parameters model used in the 'Private' experiment do not use MOT2020 training sets for training. Compared with other data sets, the MOT2020 data sets are denser with pedestrians and are more demanding on the performance of the detector.

As can be seen in Table 1, after using the Kalman filter compensation module (KC), the MOTA, IDF1 and ID switching have been significantly improved due to compensation for the missed object. However, because of unconditional compensation, some EBBoxes will still appear. Therefore, after adding the forecast correction module (FC) on this basis, the two important indicators of MOTA and IDF1 can be further improved, while only a small amount of ID switching is added.

As can be seen in Table 2, in the MOT2016 test sets, after using our tracker, the effect of the JDE model is better than the original one. Among them, IDF1 has a 3.3% increase, and MOTA has a 1.4% increase. More importantly, MT increased by 16.1% and ML decreased by 15.2%. This shows that our tracker can effectively improve tracking performance and optimize the entire model. Especially in the 2020 training sets, the improvement effect is more prominent, and various indicators have improved greatly. Among them, MOTA increased by 6.1, IDF1 increased by 11, and ID switching decreased by 7474. For the baseline model, various indicators have also been improved in MOT2016. Among them, MOTA increased by 1.1%, MT increased by 2.5%, ML decreased by 3.2%, and ID switching decreased by 41. Furthermore, it can also be seen that in the dense scene MOT2020, after using our tracker, the tracking instability problem is further alleviated, and various indicators such as MOTA, IDF1 have been improved to a certain extent. Also, the ID switch dropped by 8579

This is because the compensation tracker alleviates the problem of detector instability and makes up for the missed object tracking, so that these missed objects can be effectively tracked. Our tracker can not only accurately compensate for missed object, but also reduce unnecessary ID switching.

Table 3: 'Public' model ablation experiment. '\*' means that the model data is evaluated by motchallenge-devkit. The best result for each indicator will be bold and red.

MOT2020 Test								
Models	MOTA $\uparrow$	IDF1 $\uparrow$	MOTP $\uparrow$	MT $\uparrow$	ML $\downarrow$	FAF $\downarrow$	ID.Sw $\downarrow$	Frag $\downarrow$
Sort[8]	42.7	45.1	<b>78.5</b>	16.7%	26.2%	<b>6.1</b>	4470	17798
Ours	<b>43.3</b>	<b>45.2</b>	78.2	<b>17.6%</b>	<b>26.3%</b>	6.3	<b>2971</b>	<b>7485</b>
MOT2020 Train								
Models	MOTA $\uparrow$	IDF1 $\uparrow$	MOTP $\uparrow$	MT $\uparrow$	ML $\downarrow$	FAF $\downarrow$	ID.Sw $\downarrow$	Frag $\downarrow$
Sort[8]*	45.8	34.1	<b>87.9</b>	288	593	/	12992	/
Ours	<b>52.9</b>	<b>52.2</b>	<b>87.1</b>	<b>424</b>	<b>417</b>	/	<b>3739</b>	/

Note: The training set assessment tool does not provide the results of the FAF and Frag indicators

As can be seen in Table 3, in the MOT2020 test sets, after using the tracker of this design, the performance of Sort can be further improved. Among them, MOTA increased by 0.6%, and MT increased by 0.9%. Especially in ID switching and Frag indicators, the reductions are 1499 and 10313 respectively. In the MOT2020 training sets, the performance of our tracker has been greatly improved. Among them, MOTA increased by 7.1%, IDF1 increased by 18.1%, and ID switching decreased by 9253. In addition, it can be seen that the two tracking performance

indicators in MT and ML have also been greatly improved. This shows that the compensation tracker is very effective in data association and can further improve the tracking performance of the models.

#### 4.3 Compare with the state-of-art Models

In this part, our method will be compared with the current state-of-art multi-object tracking models. These models, including one-stage model and two-stage model, belong to the 'Private' ranking list.

**Comparative Experiment.** As can be seen in Table 4, the test results of this method on the MOT2016 and MOT2017 data sets are outstanding. And there are improvements in MOTA, IDF1 and MT and ML. In the MOT2016 test sets, the MOTA indicator is 69.8, the IDF1 indicator is 71.1, the MT indicator is 42%, and the ML indicator is 15.8%. In addition, in the MOT2017 test sets, MOTA, IDF1, MT and ML are 68.8, 70.2, 40.8%, and 17.7%, respectively.

The effect of using our tracker is more obvious on MOT2020. It can be clearly seen in Table 5 that compared with the baseline model, after using the compensation tracker, the effect

Table 4: Comparative experiment of MO20T16 and MOT2017. The best result for each indicator will be bold and red.

MOT2016 Test						
Models	MOTA ↑	IDF1 ↑	MOTP ↑	MT ↑	ML ↓	ID.Sw ↓
EAMTT[28]	52.5	53.3	78.8	19%	34.9%	910
SORTwHOD16[8]	59.8	53.8	79.6	25.4%	22.7	1423
Deep_SORT_2[4]	61.4	62.2	79.1	32.8%	18.2%	781
VMaxx[29]	62.6	49.2	78.3	32.7%	21.1%	1389
RAR16wVGG[30]	63.0	63.8	78.8	39.9%	22.1%	482
CNNMTT[14]	65.2	62.2	78.4	32.4%	21.3%	946
POI[13]	66.1	65.1	79.5	34.0%	20.8%	805
Tube_TK_POI[31]	66.9	62.2	78.5	39.0%	16.1%	1236
FairMOT[3]	68.7	70.4	80.2	39.5%	19.0%	953
Ours	69.8	71.1	80.0	42.0%	15.8%	912
MOT2017 Test						
Models	MOTA ↑	IDF1 ↑	MOTP ↑	MT ↑	ML ↓	ID.Sw ↓
SST[34]	52.4	49.5	76.9	21.4%	30.7%	8431
Tube_TK[31]	63.0	58.6	78.3	31.2%	19.9%	4137
FairMOT[3]	67.5	69.8	80.3	37.7%	20.8%	2868
Ours	68.8	70.2	80.0	40.8%	17.7%	2805

Table 5: Comparative experiment of MOT2020. The best result for each indicator will be bold and red.

MOT2020 Test								
Models	MOTA↑	IDF1↑	MOTP↑	MT↑	ML↓	FAF↓	ID.Sw↓	Frag↓
FairMOT[3]	58.7	63.7	77.2	66.3%	8.5%	24.7	6013	8140
Ours	66.0	67.0	77.8	56.3%	13.3%	9.8	2237	4154

has been greatly improved. Especially in the two comprehensive indicators in MOTA and IDF1, after using the compensation tracker, it can increase by 7.3% and 3.3% respectively. The average number of false alarms per frame FAF has dropped by 14.9% overall. Frag indicators have been greatly eased, reducing the trajectory fragmentation of 3986 object. The total number of ID Switches has dropped from 6013 to 2237. Therefore, combining the performance on the three data sets, our tracker can effectively improve the tracking performance without harming the performance of the existing models.

## 5. Conclusion

In this paper, we propose a simple compensation tracker that can be ported to other models. Although the existing detection-based tracking methods have overall preference for the effect of multi-object tracking, their problems in data association and missed detection are still prominent. The detection-based method is easy to make the tracking performance of the whole model worse because of the detector's omission. The method in this article can effectively solve this problem to a certain extent and achieve better tracking performance.

## Reference

- [1] Ren S, He K, Girshick R, et al. Faster r-cnn: Towards real-time object detection with region proposal networks[C]//Advances in neural information processing systems. 2015: 91-99.
- [2] Zhou X, Wang D, Krähenbühl P. Objects as points[J]. arXiv preprint arXiv:1904.07850, 2019.
- [3] Zhan Y, Wang C, Wang X, et al. A Simple Baseline for Multi-Object Tracking[J]. arXiv preprint arXiv:2004.01888, 2020.
- [4] Wojke N, Bewley A, Paulus D. Simple online and realtime tracking with a deep association metric[C]//2017 IEEE international conference on image processing (ICIP). IEEE, 2017: 3645-3649.
- [5] Wang Z, Zheng L, Liu Y, et al. Towards real-time multi-object tracking[J]. arXiv preprint arXiv:1909.12605, 2019.
- [6] Bochkovskiy A, Wang C Y, Liao H Y M. YOLOv4: Optimal Speed and Accuracy of Object Detection[J]. arXiv preprint arXiv:2004.10934, 2020.
- [7] Tan M, Le Q V. Efficientnet: Rethinking model scaling for convolutional neural networks[J]. arXiv preprint arXiv:1905.11946, 2019.
- [8] Bewley A, Ge Z, Ott L, et al. Simple online and realtime tracking[C]//2016 IEEE International Conference on Image Processing (ICIP). IEEE, 2016: 3464-3468.
- [9] Yu F, Wang D, Shelhamer E, et al. Deep layer aggregation[C]//Proceedings of the IEEE conference on computer vision and pattern recognition. 2018: 2403-2412.
- [10] Cao Z, Simon T, Wei S E, et al. Realtime multi-person 2d pose estimation using part affinity fields[C]//Proceedings of the IEEE conference on computer vision and pattern recognition. 2017: 7291-7299.
- [11] Newell A, Huang Z, Deng J. Associative embedding: End-to-end learning for joint detection and grouping[C]//Advances in neural information processing systems. 2017: 2277-2287.
- [12] Zhu X, Hu H, Lin S, et al. Deformable convnets v2: More deformable, better results[C]//Proceedings of the IEEE Conference on Computer Vision and Pattern Recognition. 2019: 9308-9316.
- [13] Yu F, Li W, Li Q, et al. Poi: Multiple object tracking with high performance detection and appearance feature[C]//European Conference on Computer Vision. Springer, Cham, 2016: 36-42.
- [14] Mahmoudi N, Ahadi S M, Rahmati M. Multi-target tracking using CNN-based features: CNNMTT[J]. Multimedia Tools and Applications, 2019, 78(6): 7077-7096.
- [15] Zhou Z, Xing J, Zhang M, et al. Online multi-target tracking with tensor-based high-order graph matching[C]//2018 24th International Conference on Pattern Recognition (ICPR). IEEE, 2018: 1809-1814.
- [16] Bochinski E, Eiselein V, Sikora T. High-speed tracking-by-detection without using image information[C]//2017 14th IEEE International Conference on Advanced Video and Signal Based Surveillance (AVSS). IEEE, 2017: 1-6.
- [17] He K, Gkioxari G, Dollár P, et al. Mask r-cnn[C]//Proceedings of the IEEE international conference on computer vision. 2017: 2961-2969.
- [18] Redmon J, Farhadi A. Yolov3: An incremental improvement[J]. arXiv preprint arXiv:1804.02767, 2018.
- [19] Kalman R E. A new approach to linear filtering and prediction problems[J]. 1960.
- [20] H.W.Kuhn, "The Hungarian method for the assignment problem," Naval Research Logistics Quarterly, vol. 2, pp. 83–97, 1955
- [21] Chen L, Ai H, Zhuang Z, et al. Real-Time Multiple People Tracking with Deeply Learned

Candidate Selection and Person Re-Identification[C]//2018 IEEE International Conference on Multimedia and Expo (ICME). IEEE, 2018: 1-6.

[22] Zhou X, Koltun V, Krähenbühl P. Tracking Objects as Points[J]. arXiv preprint arXiv:2004.01177, 2020.

[23] Bergmann P, Meinhardt T, Leal-Taixe L. Tracking without bells and whistles[C]//Proceedings of the IEEE international conference on computer vision. 2019: 941-951.

[24] Lu Z, Rathod V, Votell R, et al. RetinaTrack: Online Single Stage Joint Detection and Tracking[C]//Proceedings of the IEEE/CVF Conference on Computer Vision and Pattern Recognition. 2020: 14668-14678.

[25] Ciaparrone G, Sánchez F L, Tabik S, et al. Deep learning in video multi-object tracking: A survey[J]. Neurocomputing, 2020, 381: 61-88.

[26] Milan A, Leal-Taixé L, Reid I, et al. MOT16: A benchmark for multi-object tracking[J]. arXiv preprint arXiv:1603.00831, 2016.

[27] Dendorfer P, Rezatofighi H, Milan A, et al. MOT20: A benchmark for multi object tracking in crowded scenes[J]. arXiv preprint arXiv:2003.09003, 2020.

[28] Sanchez-Matilla R, Poiesi F, Cavallaro A. Online multi-target tracking with strong and weak detections[C]//European Conference on Computer Vision. Springer, Cham, 2016: 84-99.

[29] Wan X, Wang J, Kong Z, et al. Multi-object tracking using online metric learning with long short-term memory[C]//2018 25th IEEE International Conference on Image Processing (ICIP). IEEE, 2018: 788-792.

[30] Fang K, Xiang Y, Li X, et al. Recurrent autoregressive networks for online multi-object tracking[C]//2018 IEEE Winter Conference on Applications of Computer Vision (WACV). IEEE, 2018: 466-475.

[31] Pang B, Li Y, Zhang Y, et al. TubeTK: Adopting Tubes to Track Multi-Object in a One-Step Training Model[C]//Proceedings of the IEEE/CVF Conference on Computer Vision and Pattern Recognition. 2020: 6308-6318.

[32] Sun S J, Akhtar N, Song H S, et al. Deep affinity network for multiple object tracking[J]. IEEE transactions on pattern analysis and machine intelligence, 2019.

[33] Bernardin K, Stiefelhagen R. Evaluating multiple object tracking performance: the CLEAR MOT metrics[J]. EURASIP Journal on Image and Video Processing, 2008, 2008: 1-10.

[34] Peng J, Wang C, Wan F, et al. Chained-Tracker: Chaining Paired Attentive Regression Results for End-to-End Joint Multiple-Object Detection and Tracking[J]. arXiv preprint arXiv:2007.14557, 2020.

[35] Ma C, Li Y, Yang F, et al. Deep association: End-to-end graph-based learning for multiple object tracking with conv-graph neural network[C]//Proceedings of the 2019 on International Conference on Multimedia Retrieval. 2019: 253-261.

[36] Li J, Gao X, Jiang T. Graph Networks for Multiple Object Tracking[C]//The IEEE Winter Conference on Applications of Computer Vision. 2020: 719-728.

[37] Milan A, Rezatofighi S H, Dick A, et al. Online multi-target tracking using recurrent neural networks[J]. arXiv preprint arXiv:1604.03635, 2016.

[38] Feng W, Hu Z, Wu W, et al. Multi-object tracking with multiple cues and switcher-aware classification[J]. arXiv preprint arXiv:1901.06129, 2019.

[39] Shuai B, Berneshawi A G, Modolo D, et al. Multi-Object Tracking with Siamese Track-RCNN[J]. arXiv preprint arXiv:2004.07786, 2020.

- [40] Yin J, Wang W, Meng Q, et al. A Unified Object Motion and Affinity Model for Online Multi-Object Tracking[C]//Proceedings of the IEEE/CVF Conference on Computer Vision and Pattern Recognition. 2020: 6768-6777.
- [41] Huang P, Han S, Zhao J, et al. Refinements in Motion and Appearance for Online Multi-Object Tracking[J]. arXiv preprint arXiv:2003.07177, 2020.
- [42] Xu J, Cao Y, Zhang Z, et al. Spatial-temporal relation networks for multi-object tracking[C]//Proceedings of the IEEE International Conference on Computer Vision. 2019: 3988-3998.